International Journal of Mechanical, Industrial and Aerospace Sciences
ISSN: 2517-9950
Vol:10, No:7, 2016

Finite Element Analysis of Connecting Rod

Mohammed Mohsin Ali H., Mohamed Haneef

***Abstract*—**The connecting rod transmits the piston load to the crank causing the latter to turn, thus converting the reciprocating motion of the piston into a rotary motion of the crankshaft. Connecting rods are subjected to forces generated by mass and fuel combustion. This study investigates and compares the fatigue behavior of forged steel, powder forged and ASTM a 514 steel cold quenched connecting rods. The objective is to suggest for a new material with reduced weight and cost with the increased fatigue life. This has entailed performing a detailed load analysis. Therefore, this study has dealt with two subjects: first, dynamic load and stress analysis of the connecting rod, and second, optimization for material, weight and cost. In the first part of the study, the loads acting on the connecting rod as a function of time were obtained. Based on the observations of the dynamic FEA, static FEA, and the load analysis results, the load for the optimization study was selected. It is the conclusion of this study that the connecting rod can be designed and optimized under a load range comprising tensile load and compressive load. Tensile load corresponds to 360^o crank angle at the maximum engine speed. The compressive load is corresponding to the peak gas pressure. Furthermore, the existing connecting rod can be replaced with a new connecting rod made of ASTM a 514 steel cold quenched that is 12% lighter and 28% cheaper.

***Keywords*—**Connecting rod, ASTM a514 cold quenched steel, static analysis, fatigue analysis, stress life approach.

I. Introduction

THE connecting rod is subjected to a complex state of loading. It undergoes high cyclic loads of the order of 10^5 to 10^9 cycles, which range from high compressive loads due to combustion, to high tensile loads due to inertia. Therefore, durability of this component is of critical importance. Due to these factors, the connecting rod has been the topic of research for different aspects such as production technology, materials, performance simulation, and fatigue.

Webster et al. [1] performed three dimensional finite element analysis of a high-speed diesel engine connecting rod. For this analysis, they used the maximum compressive load which was measured experimentally, and the maximum tensile load which is essentially the inertia load of the piston assembly mass. The load distributions on the piston pin end and crank end were determined experimentally. They modeled the connecting rod cap separately, and also modeled the bolt pretension using beam elements and multi point constraint equations.

Mohammed Mohsin Ali H, Associate. Professor, Dept of Mechanical Engineering, Ghousia College of Engineering, Ramanagaram-562159, Karnataka, VTU, Belgaum, India, phone:09880922905; Fax: 080-27273474; (e-mail: mohsinaligce@gmail.com).

Mohamed Haneef, Principal, Dept of Mechanical Engineering, Ghousia College of Engineering, Ramanagaram, Karnataka, Academic Senate member, VTU, Belgaum, India, phone: 09845142953; fax: 080-27273474; (e-mail: profhaneef@hotmail.com).

Yoo et al. [2] used variation equations of elasticity, material derivative idea of continuum mechanics and an adjoint variable technique to calculate shape design sensitivities of stress. The results were used in an iterative optimization algorithm, steepest descent algorithm, to numerically solve an optimal design problem. The focus was on shape design sensitivity analysis with the application to the example of a connecting rod. The stress constraints were imposed on principal stresses of inertia and firing loads. But, fatigue strength was not addressed. The other constraint was the one on thickness to bind it away from zero. They could obtain 20% weight reduction in the neck region of the connecting rod.

Folgar et al. [3] developed a fiber FP/Metal matrix composite connecting rod with the aid of FEA, and loads obtained from kinematic analysis. Fatigue was not addressed at the design stage. However, prototypes were fatigue tested. The investigators identified design loads in terms of maximum engine speed, and loads at the crank and piston pin ends. They performed static tests in which the crank ends and the piston pin end failed at different loads. Clearly, the two ends were designed to withstand different loads.

Serag et al. [4] developed approximate mathematical formulae to define the connecting rod weight and cost as objective functions and also the constraints. The optimization was achieved using a Geometric Programming technique. Constraints were imposed on the compression stress, the bearing pressure at the crank and the piston pin ends. Fatigue was not addressed. The cost function was expressed in some exponential form with the geometric parameters.

Imahashi et al. [5] presented a method to consider the fatigue life as a constraint in optimal design of structures. They also demonstrated the concept on a SAE key whole specimen. El-Sayed and Lund [6] conducted constant amplitude, load-controlled component axial fatigue tests on powder forged (PF) connecting rods. They reported that the factors which affect fatigue strength in PF connecting rod are hardness of the material, depth of decarburized layer, metallurgical structure, density, and surface roughness. They concluded that hardness has a large impact on fatigue strength. The fatigue properties were also compared to SAE 1055 steel. The comparison also showed that a major cost difference between hot forging and PF connecting rod is in machining, and that the energy saving for PF connecting rod, which is one half of that for the forged steel, is also mainly due to the machining process. However, in spite of the higher raw material weight for the steel forged connecting rod, the raw material cost is significantly lower than the PF connecting rod raw material. Sarihan and Song [7] presented a method to consider fatigue life as a constraint in optimal design of structures. They also demonstrated the concept on a SAE key

hole specimen. Athavale and Sajanpawar [8], for the optimization of the wrist pin end, used a fatigue load cycle consisting of compressive gas load corresponding to maximum torque and tensile load corresponding to maximum inertia load. Evidently, they used the maximum loads in the whole operating range of the engine. To design for fatigue, modified Goodman equation with alternating octahedral shear stress and mean octahedral shear stress was used. For optimization, they generated an approximate design surface, and performed optimization of this design surface. The objective and constraint functions were updated to obtain precise values. This process was repeated till convergence was achieved. They also included constraints to avoid fretting fatigue.

In [9], the mappings involved in the system comprise firstly, mapping between the top level feature representations associated with different viewpoints; for example for the geometric simplification and addition of boundary conditions associated with moving from a design model to an analysis model, and secondly mapping between the top level and the middle level representations in which the feature model is transformed into the executable representation. Because an executable representation is used as the intermediate layer, the low level evaluation can be active. This multi-level modelling approach will be investigated for the design automation with a feature-based model.

Hippoliti et al. [10] reported computational strategy used in Mercedes-Benz by using examples of engine components. In their opinion, 2D FE models can be used to obtain rapid trend statements, and 3D FE models for more accurate investigation. The various individual loads acting on the connecting rod were used for performing simulation and actual stress distribution was obtained by superposition. The loads included inertia load, firing load, the press fit of the bearing shell, and the bolt forces.

Sonsino et al. [11] have reported the design methodology for connecting rod which incorporates optimization technique. However, neither the details of optimization nor the load under which optimization was performed were discussed. Two parametric FE procedures using 2D plane stress and 3D approach developed by the author were compared with the experimental results and shown to have good agreements. The optimization procedure they developed was based on the 2D approach.

II. Experimental Details

A. Finite Element Modeling and Analysis of Connecting Rod

Fig. 1 represents the connecting rod model developed by using CATIA software. The geometry is built in sketcher and layer extruded to three dimensional parts in the part modeler to get three dimensional representations. Material color codes are used to represent the problem. Fig. 2 shows the connecting rod modeled with CATIA software. CATIA sketcher, part modeler and assemblers are used for building the geometry. CATIA is a solid/surface modeling software in the industry, and various modeling and assembly options are available to build the geometries. Also, geometrical dimensioning and tolerances can be provided for the modeled parts. Connecting rod was modeled was modeled by using CATIA software. The model is imported in SolidWorks and then the mechanical characteristics of the connecting rod are established for the three different materials. These properties are shown in Table I. The three dimensional model of the connecting rod is shown in Fig. 2.

Fig. 1 Individual component representation in three dimensional space

Fig. 2 Three Dimensional CATIA model of Connecting rod

B. Material Properties

Most of the research is based on use of alternate materials for connecting rods so as to reduce the weight by enhanced material properties. To study the behavior of the connecting rod model, forged steel, powder forged and ASTM a-514 cold quenched materials are used for the analysis.

C. Material Deformation and Fatigue Behaviors

Monotonic tension tests performed on the test specimens using test methods specified by ASTM Standard. Table I summarizes the monotonic tensile test results for forged steel, powder metal and ASTM a-514 material. As can be seen from this table, the yield strength of forged steel is 17% higher than that for the powder metal, whereas the yield strength of ASTM a-514 materials is 10% higher than forged steel. The ultimate tensile strength of the forged steel is 8% higher than that for the powder metal, and the ultimate tensile strength of the ASTM a-514 material is 2% higher than that for the forged steel. Table I shows the summary of mechanical properties of three materials.

Superimposed monotonic tension curves of forged steel and powder metal are shown in Fig. 3. Cyclic stress strain data obtained from the constant amplitude strain controlled fatigue tests were also used to determine the steady-state cyclic deformation response. The cyclic stress-strain curve reflects the resistance of a material to cyclic deformation and can be vastly different from the monotonic stress-strain curve. Superimposed cyclic curves of the three materials are also shown in Fig. 3. This figure shows cyclic softening behavior for forged steel. The powder metal initially cyclically softens, but then it cyclically hardens at strain amplitude higher than 0.5%. The cyclic deformation properties listed in Table II indicate slightly higher cyclic yield strength of the ASTM a-514 steel, as compared with the powder metal and forged steel.

TABLE I
SUMMARY OF MECHANICAL PROPERTIES

Properties	Forged Steel	Powder Forged	ASTM a-514 steel
Modulus of Elasticity (GPa)	201	199	210
Poison's ratio	0.3	0.3	0.3
Yield stress(MPa)	690	588	760
Ultimate Tensile Strength	938	866	956
Percent elongation, %EL	24 %	23%	18%
Percent reduction in area, %RA	42%	23%	35%
Strength coefficient, K (MPa)	1,400	1,379	1760
True fracture strength, σ_f (MPa)	1266	994	1150

S-N material behavior is described by the Basquinequation:

$$S_{Nf} = \sigma_f (2N_f)^b. \quad (1)$$

where σ_f and b are the fatigue strength coefficient and exponent, respectively. Comparison of long-life fatigue strength, S_{Nf}, which is defined as the fatigue strength at10^6 cycles, shows that the fatigue strength of forged steel is 27% higher than that for the powder metal, whereas the ASTM a-514 steel has higher fatigue strength of 10% compared to forged steel. Fig. 4 indicates that this results in about an order of magnitude longer life than the forged steel and powder metal.

Superimposed strain-life curves of the three materials are shown in Fig. 5. From this figure, it can be seen that in the long life regime (high cycle fatigue), the ASTM a-514 steel has got good life regime than the forged steel and powder metal material, while in the short life regime (low cycle fatigue) the difference is smaller. However, it should be kept in mind that for a connecting rod, which is subjected to many millions of stress cycles, the high cycle regime is of primary interest.

D.Loading and Boundary Conditions

In this study, four finite element models were analysed. FEA for both tensile and compressive loads were conducted. Two cases were analysed for each problem; one with load applied at the crank end and restrained at the crank end.

1. Compressive Loading Stress

Crank End $\boldsymbol{P_0 = \frac{27090}{(24.35)(17.3)(\sqrt{3})} = 37.128\ MPa}$

Piston End $\boldsymbol{P_0 = \frac{27090}{(12.15)(17.702)(\sqrt{3})} = 72.702\ MPa}$

2. Tensile Loading Stress

Crank End $\boldsymbol{P_0 = \frac{27090}{(24.35)(17.3)(\pi/2)} = 40.939\ MPa}$

Piston End $\boldsymbol{P_0 = \frac{27090}{(12.15)(17.702)(\pi/2)} = 80.18\ MPa}$

Since the analysis is linearly elastic, for static analysis the stress, displacement, and strain are proportional to the magnitude of the load. Therefore, the obtained results from FEA readily compare with the above values.

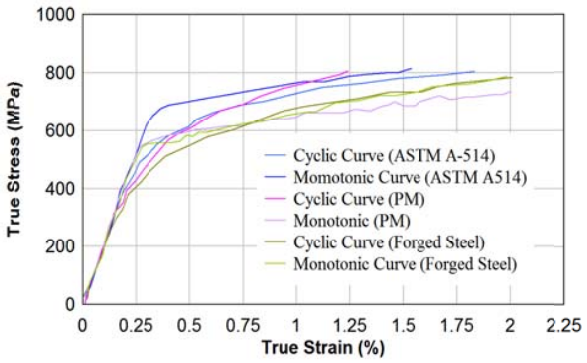

Fig. 3 Superimposed monotonic and cyclic stress strain curves of forged steel, powder metal and ASTM a-514 materials

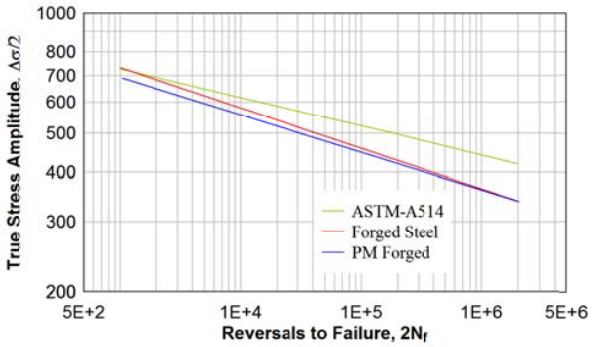

Fig. 4 Superimposed curves of true stress amplitude versus reversals to failure for three materials

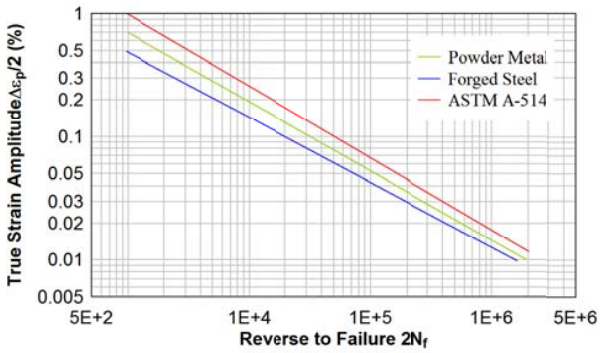

Fig. 5 Superimposed curves of true strain amplitude versus reversals to failure for three materials

E. FEA Results

The load analysis was carried out to obtain the loads acting on the connecting rod at any given time in the loading cycle and to perform FEA. Most investigators have used the static axial loads for the design and analysis of connecting rods. In the static analysis, von Mises stress, critical locations observed under tension and compression loadings at the piston and crank ends. The most highly stressed areas are in the transition regions between the shank and the crank end, as well as the shank and the pin end. Stresses are all symmetric over the entire rod, since geometry and loading were symmetrical.

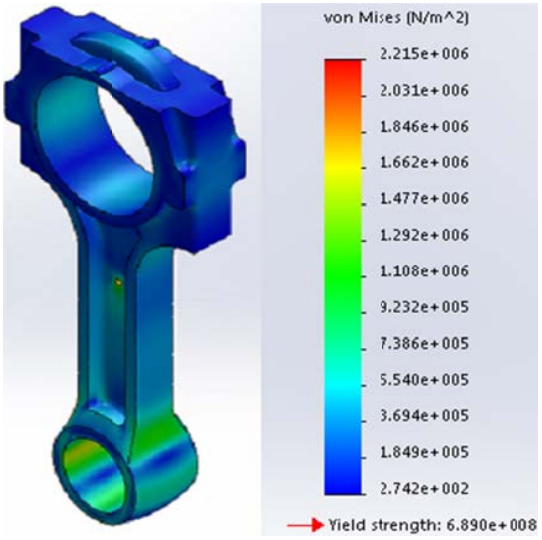

Fig. 6 Connecting Rod-Tension-Stress (von Mises stress)von Mises Stress is maximum at node No. 160628and its value is2.12 MPa

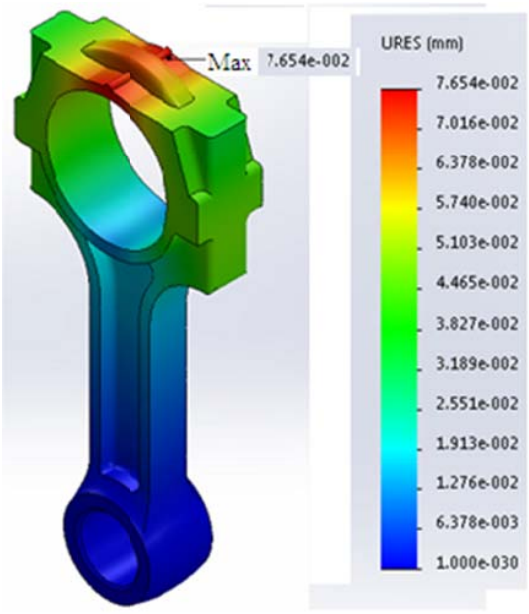

Fig. 7 Connecting Rod Displacement, Max displacement is 0.0765383 mm at node: 101773

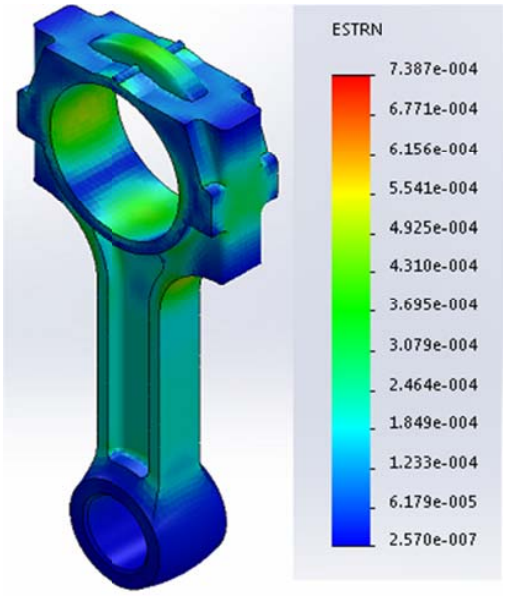

Fig. 8 Connecting Rod-Tension-Strain, Max strain is 0.000738672 at Element: 11885 Min stain is 2.57007e-007 at Element No. 50881

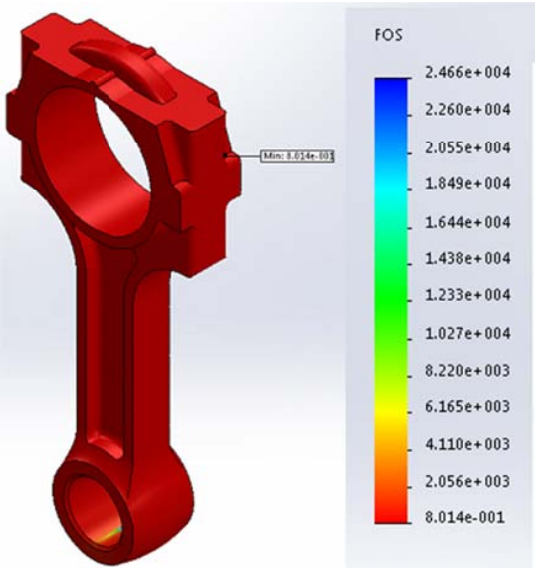

Fig. 9 Connecting Rod-Tension-Factor of Safety

TABLE II
VON MISES STRESSES UNDER TENSILE AND COMPRESSIVE LOADS IN THE SHANK REGION

Node label	Tensile Load = 27.09 kN: Load at Crank End von Mises Stress (MPa)	Tensile Load = 27.09 kN: Load at Piston End von Mises Stress (MPa)	%Diff	Compressive Load = 27.09 kN: Load at Crank End von Mises Stress (MPa)	Compressive Load = 27.09 kN: Load at Piston End von Mises Stress (MPa)	%Diff
38206	199.3	195.7	1.8	199.9	200.1	-0.1
5824	207	202.3	2.27	205.8	204.9	0.43
32452	199.3	195.7	1.8	199.9	200.1	-0.1

Validation of model is done, and Table II shows the von Mises stresses under tensile and compressive loading in the shank region. First by restraining the crank end, a load of 27.09 kN was applied at the pin end and secondly the pin end was restrained and the same load was uniformly distributed at the crank end. The above table justifies the model of FEA since the connecting rod is symmetric about its axis the symmetric nodes are having the same stress.

TABLE III
SUMMARY OF RESULTS

Name	Scope	Type	Design Life	Min	Max	Alert Criteria
Life	Model	Life		10^6	10^6	None
Damage	Model	Damage	1.0×10^9	1,000	1,000	None
Safety Factor	Model	Safety Factor	1.0×10^9	1.13	15.0	None
Biaxiality Indication	Model	Biaxiality Indication		-1.0	0.97	None
Equivalent Alternating Stress	Model	Equivalent Reversed Stress		0.01 Mpa	76.22 Mpa	None

Summary of the results obtained are shown in Table III. It can be seen from the table that minimum value of safety factor for design life of 1.0x109 cycles is1.13 and maximum is 15.0. Similarly, the minimum value of equivalent alternating stress is 0.01 MPa and maximum is 76.22 MPa.

III. CONCLUSION

The effects of material properties on fatigue and optimization of automotive connecting rods were investigated. From tensile tests and monotonic deformation curves, it is concluded that ASTM a-514 steel is considerably stronger and more ductile than forged steel and Powder metal. ASTM a-514 steel has higher fatigue strength of 10 % when compared with forged steel and 27% higher when compared to powder metal respectively.

The cyclic yield strength of ASTM a-514 steel is found to be 80% and 75% of forged steel, respectively. The cyclic strain hardening exponent of ASTM a-514 steel was 59% and 55% of the forged steel, respectively. These indicate the higher cyclic strength of ASTM a-514 steel against yielding, and its higher resistance to plastic deformation.

The proposed material alternatives provide higher fatigue strength for the component. Manufacturability and cost are the two other main issues that are critical to the final selection of the replacing material. Limited weight saving is achieved by replacing the potential alternative materials, mainly due to geometrical constraints. If comprehensive changes to the geometry are allowed or for other components with fewer constraints, the weight saving will be more significant.

REFERENCES

[1] Webster, W. D., Coffell R., and Alfaro D., "A Three Dimensional Finite Element Analysis of a High Speed Diesel Engine Connecting Rod," SAE Technical Paper Series, Paper No. 831322,1983,
[2] Yoo, Y. M., Haug, E. J., and Choi, K. K., 1984, "Shape optimal design of an engine connecting rod," Journal of Mechanisms, Transmissions, and Automation in Design, Transactions of ASME, Vol. 106, pp. 415-419,1984.
[3] Folgar, F., Wldrig, J. E., and Hunt, J. W. "Design, Fabrication and Performance of Fiber FP/Metal Matrix Composite Connecting Rods,"
[4] Serag, S., Sevien, L., Sheha, G., and El-Beshtawi, I., "Optimal design of the connecting-rod", Modelling, Simulation and Control, B, AMSE Press, Vol. 24, No. 3, pp. 49-63,1989.
[5] Imahashi, K., Tsumuki, C., and Nagare, I., 1984, "Development of powder-forged connecting rods," *SAE Technical Paper* 841221, pp. 1-7.
[6] El-Sayed, M. E. M., and Lund, E. H., "Structural optimization with fatigue life constraints," Engineering Fracture Mechanics, Vol. 37, No. 6, pp. 1149-1156,1990.
[7] Sarihan, V. and Song, J., "Optimization of the Wrist Pin End of an Automobile Engine Connecting Rod With an Interference Fit," Journal of Mechanical Design, Transactions of the ASME, Vol. 112, pp. 406-412,1990.
[8] Athavale, S. and Sajanpawar, P. R. "Studies on Some Modelling Aspects in the Finite Element Analysis of Small Gasoline Engine.SAE Technical Paper Series, Paper No. 911271,1991.
[9] Balasubramaniam, B., Svoboda, M., and Bauer, W. "Structural optimization of I.C. engines subjected to mechanical and thermal loads," Computer Methods in Applied Mechanics and Engineering, Vol. 89, pp. 337-360,1991.
[10] Hippoliti, R., "FEM method for design and optimization of connecting rods for small two-stroke engines," Small Engine Technology

[11] Sonsino, C. M., and Esper, F. J, "Fatigue Design for PM Components," EuropeanPowder Metallurgy Association (EPMA),1994.